molecular pharmaceutics

Article

pubs.acs.org/molecularpharmaceutics

Membrane and Nuclear Permeabilization by Polymeric pDNA Vehicles: Efficient Method for Gene Delivery or Mechanism of Cytotoxicity?

Giovanna Grandinetti,[†] Adam E. Smith,[†] and Theresa M. Reineke*[,†,‡]

[†]Department of Chemistry, Virginia Polytechnic Institute and State University, Blacksburg, Virginia 24061, United States

[‡]Department of Chemistry, University of Minnesota, Minneapolis, Minnesota 55455, United States

Supporting Information

ABSTRACT: The aim of this study is to compare the cytotoxicity mechanisms of linear PEI to two analogous polymers synthesized by our group: a hydroxyl-containing poly(L-tartaramidoamine) (T4) and a version containing an alkyl chain spacer poly(adipamidopentaethylenetetramine) (A4) by studying the cellular responses to polymer transfection. We have also synthesized analogues of T4 with different molecular weights (degrees of polymerization of 6, 12, and 43) to examine the role of molecular weight on the cytotoxicity mechanisms. Several mechanisms of polymer-induced cytotoxicity are investigated, including plasma membrane permeabilization, the formation of potentially harmful polymer degradation products during transfection including reactive oxygen species, and nuclear membrane permeabilization. We hypothesized that since cationic polymers are capable of disrupting the plasma membrane, they may also be capable of disrupting the nuclear envelope, which could be a potential mechanism of how the pDNA is delivered into the nucleus (other than nuclear envelope breakdown during mitosis). Using flow cytometry and confocal microscopy, we show that the polycations with the highest amount of protein expression and toxicity, PEI and $T4_{43}$, are capable of inducing nuclear membrane permeability. This finding is important for the field of nucleic acid delivery in that direct nucleus permeabilization could be not only a mechanism for pDNA nuclear import but also a potential mechanism of cytotoxicity and cell death. We also show that the production of reactive oxygen species is not a main mechanism of cytotoxicity, and that the presence or absence of hydroxyl groups and polymer length play a role in polyplex size and charge in addition to protein expression efficiency and toxicity.

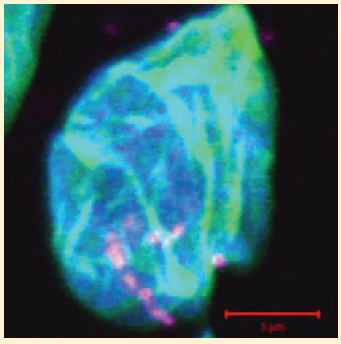

KEYWORDS: *gene delivery polymers, toxicity, polyethylenimine, apoptosis, PGAAs, glycopolymer*

INTRODUCTION

The delivery of nucleic acids has great potential to alleviate many disorders, but finding a safe and effective vehicle has proven to be a challenge. Viruses have the innate ability to deliver genetic cargo to target cells and are currently being used in clinical trials. However, they are not ideal vehicles; they have been shown to elicit unwanted immune responses, have a small capacity, are not versatile for carrying a variety of nucleic acid forms, and are difficult to modify.[1] Cationic polymer-based DNA vehicles have been developed to combat some of the problems associated with viral vectors;[2] many of these polymers are able to interact with DNA to form polymer−DNA complexes (polyplexes) of 100 nm or less.[3] Studying nanosystems for use as delivery vehicles has increased steadily in recent years, and the field of nanotechnology is predicted to become a trillion dollar industry by 2015.[4] Despite the recent surge in interest for the development of effective polymer therapeutics, the mechanisms of polymer-mediated DNA delivery and particularly of their cytotoxicity remain largely unknown.

Polyethylenimine (PEI) and PEI-based systems have undergone extensive study for their use as DNA delivery vehicles.[5−7] PEI is able to deliver its cargo DNA effectively, but its high cytotoxicity has hampered its use *in vivo*.[8−10] In an effort to create a safe and efficient cationic polymer vehicle for DNA delivery, our group has synthesized a series of poly(glycoamidoamine)s (PGAAs), which contain carbohydrate moieties along with short PEI-like polyamines repeated along the backbone.[11−13] These polymers display significantly lower toxicity than PEI, and previous research in our group has shown that these PGAAs undergo different mechanisms of cellular internalization and intracellular trafficking.[14,15] Further studies performed by our group show the presence of a carbohydrate moiety within the backbone of these polyamides facilitates their rapid degradation at physiological conditions.[16] Although less toxic than PEI, a small fraction of cell death still occurs with PGAA-transfected cells.

The aim of this study is to examine the role that polymer structure plays in transfection and toxicity during the polyplex

Received: July 22, 2011
Revised: November 14, 2011
Accepted: December 18, 2011
Published: December 19, 2011

transfection process. In particular, to yield insight into the mechanisms of toxicity for this class of polymers, we have focused on comparing one degradable PGAA structure, T4, consisting of an L-tartarate monomer copolymerized with pentaethylenehexamine to an analogous model lacking hydroxyls, $A4_{42}$, which does not degrade. We also investigate the role of T4 polymer length on the biological properties and utilize linear PEI as a control in these experiments. Understanding the differences in the mechanism of toxicity for these three vehicle structures is important to the general field of drug and nucleic acid delivery to enable rational vehicle design for high transfection and low toxicity. To this end, cells were transfected with five different polymer structures: a commercially available linear PEI (JetPEI), three different lengths of polymer T4 ($T4_6$, $T4_{12}$, and $T4_{43}$; subscript corresponding to the degree of polymerization), and polymer $A4_{42}$, which had a comparable degree of polymerization and molecular weight to $T4_{43}$. This study allowed us to examine the role of polymer molecular weight, the presence of hydroxyl groups, and the polymer charge density on polyplex toxicity and transfection efficiency with Hela cells. Flow cytometric analysis revealed that the polymers tested were able to decrease mitochondrial membrane potential and increase phosphatidylserine exposure, two hallmark signs of apoptosis, as well as increase plasma membrane permeability four hours after transfection. Herein, it is demonstrated that the presence or absence of a carbohydrate moiety and polymer length influence polyplex cytotoxicity to a large degree. We show that longer polymers are able to induce mitochondria depolarization and phosphatidylserine exposure to a larger degree and earlier in transfection than shorter polymers. Furthermore, when comparing two polymers of similar molecular weight, the carbohydrate-containing $T4_{43}$ and the polymer devoid of carbohydrate moieties, $A4_{42}$, we see differences in cellular toxic response. $T4_{43}$ displays higher toxicity 48 h after transfection, and induces higher phosphatidylserine exposure within 4 h of transfection. We also observe differences in the polyplexes themselves, with $A4_{42}$ polyplexes being more positively charged and having a smaller hydrodynamic radius than $T4_{43}$ polyplexes.

MATERIALS AND METHODS

Dulbecco's Modified Eagle Medium (DMEM), cell culture media supplements, phosphate-buffered saline (PBS) and fetal bovine serum (FBS) were purchased from Gibco (Carlsbad, CA). The mitochondrial membrane potential probe 1,1′,3,3,3′,3′-hexamethylindodicarbocyanine iodide (DiIC(1)5), phosphatidylserine exposure probe Annexin V, and viability probe propidum iodide were purchased from Molecular Probes (Eugene, OR) and used according to the manufacturer's protocol. Linear PEI (JetPEI) was purchased from PolyPlus Transfections (Illkirch, France) and used according to the manufacturer's protocol.

Synthesis and Characterization of Polymers. To study the effect of polymer length on cytotoxicity for the T4 analogues, three different molecular weight polymers were synthesized by varying polymerization reaction times. The T4 was synthesized using a modified procedure similar to a previously described method;[11] to create short T4 ($T4_6$) with a degree of polymerization (DP) of 6, the monomers were reacted for 4 days; to synthesize the intermediate-sized T4 ($T4_{12}$), the polymerization was carried out for 6 days; and in order to synthesize the longer T4 polymers ($T4_{43}$), the monomers were polymerized for 8 days. $A4_{42}$ was synthesized as previously described.[16] Gel permeation chromatography (GPC) was used to determine the average molecular weight (M_n) and polydispersity indices (PDIs) for the T4 and $A4_{42}$ polymers using an aqueous eluent of 1.0 wt % acetic acid/0.1 M Na_2SO_4. A flow rate of 0.3 mL/min, Eprogen Inc. columns [CATSEC1000 (7μ, 50 × 4.6), CATSEC100 (5μ, 250 × 4.6), CATSEC300 (5μ, 250 × 4.6), and CATSEC1000 (7μ, 250 × 4.6)], a Wyatt HELEOS II light scattering detector (λ = 662 nm), a ViscoStar II differential viscometer, and an Optilab rEX refractometer (λ = 658 nm) were used. Astra V (version 5.3.4.18, Wyatt Technologies) was used for the determination of M_n, PDI, Mark–Houwink–Sakurada values, and the dn/dc of the polymers.

Polyplex Characterization. Polyplexes were formed by adding 150 μL of polymer solution to 150 μL of plasmid DNA (pDNA) (0.02 μg/μL) at a nitrogen to phosphate (N/P) ratio [ratio of the amines (excluding amide nitrogens) in the polymer repeat unit to phosphate groups on pDNA] of 20 for the PGAAs. Polyplexes formed with PEI were formed the same way except an N/P ratio of 5 was used. Polyplexes were incubated for one hour at room temperature, and then diluted with 600 μL of water prior to size and charge measurements. Polyplex size was measured on a Zetasizer (Nano ZS) (Malvern Instruments, Malvern, U.K.) at 37 °C using dynamic light scattering with a laser wavelength of 633 nm. Zeta potentials of the polyplexes were subsequently measured on the same instrument. Three polyplex solutions were used for each measurement; data is presented as means ± standard deviation.

Protein Expression. Protein expression was measured using a luciferase reporter gene assay 48 h after transfection as previously described.[11] Briefly, HeLa cells were seeded at a density of 50,000 cells/well in a 24 well plate. Polyplexes were formed as described above for the polyplex characterization studies, except 600 μL of serum-free media (OptiMEM, Gibco, Carlsbad, CA) was added to each polyplex solution instead of water. Cells were transfected using 1 μg of pDNA per well. Where indicated, 5 μM of camptothecin (Sigma) was added to cells with polyplexes for 4 h, then the camptothecin-containing media was aspirated off, cells were washed with PBS, and 1 mL of 10% FBS DMEM was added to each well. For the camptothecin studies, transfection efficiency was measured 24 h after transfection. All luciferase data were normalized to the cells only control, and data are expressed as relative light units (RLU) per milligram of protein.

Flow Cytometry. HeLa cells were seeded at a density of 250,000 cells/well in a 6 well plate in Dulbecco's modified Eagle medium (DMEM) supplemented with 10% fetal bovine serum, 100 μg/mL streptomycin, 0.25 μg/mL amphotericin, and 100 units/mg penicillin. The cells were incubated at 37 °C and 5% CO_2 for 24 h. After the 24 h cell incubation, 500 μL of each polyplex solution was made by adding 250 μL of polymer solution at indicated N/P ratios to 250 μL of 0.02 μg/μL pDNA solution. The polyplex solution was allowed to incubate for one hour at room temperature. After one hour, 1 mL of serum-free media (OptiMEM) was added to the 500 μL polyplex solutions. Cells were washed with PBS (1 mL/well), and 1.5 mL of transfection solution was added to each well (5 μg of pDNA/well). Transfections were performed in triplicate. Cells were allowed to transfect for indicated time periods, then transfection media was aspirated off, and cells were washed twice with PBS, trypsinized, and pelleted at 200 × g for 10 min. Cells were resuspended in 1 mL of PBS, pelleted, resuspended

in 500 μL of PBS, and analyzed using a BD FACSCanto II (Becton-Dickenson, San Jose, California) flow cytometer.

Apoptosis Detection. The dyes DiIC(1)5 and Annexin V conjugated to Alexa Fluor 488 were used to monitor mitochondrial membrane potential and phosphatidylserine exposure, respectively, according to the manufacturer's protocol. Propidium iodide was added to cells prior to flow cytometry analysis to study plasma membrane permeability according to the manufacturer's protocol. Transfections were done in triplicate. A minimum of 20,000 events was collected for each sample.

Cellular Uptake. For cellular uptake experiments, polyplexes were formed using Cy5-labeled pDNA and the increase in Cy5 fluorescence in HeLa cells was measured two hours after transfection using flow cytometry. Cells were transfected in the presence or absence of 0.9 mM ethylene glycol tetraacetic acid (EGTA) to chelate extracellular calcium. A minimum of 10,000 events was collected for each sample.

Nucleus Isolation. HeLa cells were seeded and transfected in 6 well plates as described above. Four hours after transfection, each sample was pelleted and resuspended in 500 μL of OptiMEM containing 2 mM DL-dithiothreitol (DTT), 40 μg/mL digitonin, and 1 μg/mL protease inhibitor cocktail (Sigma Aldrich, St. Louis, MO). Cells were incubated on ice for 5 min. After incubation, nuclei were pelleted *via* centrifugation at 2000*g*, 4 °C for 10 min. Nuclei were resuspended in 500 μL of OptiMEM containing 2 mM DTT and incubated on ice for 10 min to ensure complete isolation of the nuclei and separation from the cytosolic components. After the 10 min incubation, nuclei were pelleted as described above and resuspended in 500 μL of PBS for flow cytometric analysis.

Nuclear Uptake. After nuclear isolation, the nuclei were analyzed for Cy5 and propidium iodide fluorescence *via* flow cytometry as described above. To determine whether polyplexes were inside the nuclei or adhered to the surface of the nuclei, confocal microscopy was performed on the samples analyzed by flow cytometry. The nuclei were repelleted after flow cytometric analysis and resuspended in 1 mL of 4% paraformaldehyde solution. Nuclei were fixed for 15 min at room temperature, after which nuclei were pelleted, resuspended in 1 mL of PBS, and deposited on PLL-coated coverslips. Nuclei were allowed to incubate on coverslips overnight at 4 °C before being mounted on microscopy slides using ProLong Gold Antifade reagent (Molecular Probes, Eugene, OR) according to the manufacturer's protocol. Nuclei were analyzed on a Zeiss LSM 510 META confocal microscope. Z-stacks of each image were collected using overlapping 0.39 μM slice thicknesses and Zeiss Zen 2009 software. Fluorescence for each z-stack slice in the microscopy images was quantified using the software ImageJ.[17]

Confocal Microscopy. HeLa cells were grown on PLL-coated coverslips in a 12 well plate for 48 h before being transfected. The cells were seeded at 15,000 cells/well. After the 48 h incubation, the medium was aspirated off, cells were washed with 1 mL of PBS per well, and 1 mL of OptiMEM was added to each well. Polyplexes were formed as described above except 50 μL of polymer solution was added to 50 μL of 0.02 μg/μL Cy5-labeled plasmid DNA solution, giving a total of 100 μL of transfection solution per well (1 μg of pDNA/well). The 100 μL of transfection solution was added on top of the 1 mL of OptiMEM in each well, the plate was swirled to give even distribution of polyplexes, and the cells were incubated at 37 °C and 5% CO_2 for 30 min. After transfecting for 30 min, the polyplexes and OptiMEM were aspirated off, wells were washed with 1 mL of PBS, and 1 mL of 10 μg/mL Alexa Fluor 488 wheat germ agglutinin (WGA) (Molecular Probes, Eugene, OR) in Hanks buffered salt solution (HBSS) was added to each well. Cells were incubated with the labeled WGA for 15 min at room temperature, after which time the WGA was aspirated off and cells were washed twice with 1 mL of PBS in each well and fixed using 4% paraformaldehyde at room temperature for 15 min. After fixation, cells were washed three times with PBS and nuclei were stained using 4′,6-diamidino-2-phenylindole, dilactate (DAPI) (Molecular Probes, Eugene, OR), and mounted using ProLong Gold Antifade Reagent (Molecular Probes, Eugene, OR) according to the manufacturer's protocol. The slides were dried overnight in the dark before being sealed with clear nail polish and imaged using confocal microscopy.

Immunostaining of Lamin A. HeLa cells were grown on coverslips and transfected as described above. Four hours after transfection, cells were fixed in 4% paraformaldehyde at room temperature for 15 min. After fixation, cells were washed three times with PBS (1 mL of PBS per well each wash) and permeabilized using 0.25% Triton X-100 for 15 min at room temperature. Cells were then washed with PBS three times, leaving the PBS in the wells for five minutes for each wash. The cells were then blocked using a 1% bovine serum albumin (BSA) solution in PBS for 45 min at room temperature. After blocking, a 1:2000 solution of rabbit polyclonal lamin A antibody (Abcam, Cambridge, MA) in 1% BSA/PBS was added to the cells. Cells were incubated with the primary antibody for one hour at room temperature, after which time the antibody solution was aspirated off, and a 5 μg/mL solution of goat anti-rabbit secondary antibody conjugated to Alexa Fluor 488 (Molecular Probes, Eugene, OR) in 1% BSA/PBS was added to coverslips in a humidified chamber. After incubating with the secondary antibody for one hour at room temperature, coverslips were washed three times with 1 mL of PBS/well, and the PBS was allowed to stay on coverslips for 5 min each wash. After the third PBS wash, coverslips were stained with DAPI (Molecular Probes, Eugene, OR) according to the manufacturer's protocol. Coverslips were then washed twice with 600 μL of PBS and mounted on to microscopy slides using ProLong Antifade Gold reagent (Molecular Probes, Eugene, OR) according to the manufacturer's protocol. Microscopy slides were dried horizontally in the dark overnight, then sealed with clear nail polish and imaged using confocal microscopy.

Nuclear Envelope Permeability in a Cell-Free System. Nuclei were isolated from HeLa cells as described above and added to a 12 well plate at a density of 50,000 nuclei/well. Polyplexes were formed as described above (50 μL of polymer solution was added to 50 μL of 0.02 μg/μL Cy5-labeled plasmid DNA solution) and added to the nuclei in 1 mL of OptiMEM. The nuclei were incubated at 37 °C and 5% CO_2 for 4 h, after which 200 μL of a 0.4% trypan blue solution (Gibco, Carlsbad, CA) was added to each well. The nuclei were then imaged using an EVOS fl digital inverted fluorescence microscope (Advanced Microscopy Group, Bothell, WA). Images were quantified using the software ImageJ.[17]

MTT Assay. Cells were plated at a density of 50,000 cells/well in a 24 well plate. The cells were grown on the plate for 24 h prior to transfection. Polyplexes were formed using the same procedure as that used for size and zeta potential measurements, except 600 μL of OptiMEM was used to dilute the polyplex solutions instead of water. Cells were transfected in triplicate with 1 μg of plasmid DNA added to each well. At the

indicated time points, polyplex solutions were aspirated off, cells were washed with 0.5 mL of PBS per well, and 1 mL of DMEM containing 10% FBS and 0.5 mg/mL of MTT reagent (Molecular Probes, Eugene, OR) was added to cells. Cells were incubated with the MTT-containing medium for 1 h at 37 °C, then the medium was aspirated off, cells were washed with PBS as described above, and 600 μL of DMSO was added to each well. Cells were incubated on a shaker for 15 min to ensure even distribution of the purple formazan. After the shaking incubation, 200 μL was pipetted out of each well and into a clear 96 well plate, and then analyzed for absorbance at 570 nm using a Tecan GENios Pro plate reader (Tecan U.S., Research Triangle Park, NC).

ROS Detection. Intracellular reactive oxygen species (ROS) were detected using the fluorescent dye 2′,7′-dichlorodihydrofluorescein diacetate (H_2DCDFA) (Molecular Probes, Eugene, OR). HeLa cells were plated on 6 well plates at a density of 250,000 cells/well. Cells were transfected in 6 well plates as described above. At the indicated time points, polyplexes were aspirated off, cells were washed with PBS, and 1 mL of a 10 μM solution of H_2DFDFA in PBS was added to each well. Hydrogen peroxide (H_2O_2) was used at a concentration of 100 μM as a positive control and was added with the dye. Cells were incubated with the dye at 37 °C for 30 min. After the incubation, the dye was aspirated off and cells were washed with PBS and trypsinized using phenol-red free trypsin. Cells were pelleted at 200 × *g*, 4 °C for 10 min, and each sample was resuspended in 500 μL of PBS. H_2DCDFA fluorescence was measured using flow cytometry, and a minimum of 20,000 events were collected for each sample.

Statistical Analysis. All data are presented as mean ± standard deviation. Measurements were performed in triplicate unless otherwise noted. For statistical analysis of data, the software JMP was used (SAS Institute Inc., Cary, NC) and means were compared using the Tukey–Kramer HSD method, with $p < 0.05$ being considered as statistically significant.

RESULTS

Synthesis and Characterization of T4 Polymers. To examine the role that polymer length has on cytotoxicity, three different degrees of polymerization (DPs) of T4 were synthesized by varying the polymerization times from 4 to 8 days using a previously published method.[11] GPC with a triple detection system (viscometry, static light scattering, and refractive index) was used to analyze each of the polymers for molecular weight, polydispersity, and polymer solution structure (MHS parameter between 0.6 and 0.8 denotes a linear, randomly coiled polymer structure).[18] The results are shown in Table 1.

Table 1. Molecular Weight (M_w), Polydispersity Index (M_w/M_n), Mark–Houwink–Sakurada Parameter (MHS (α)), and Degree of Polymerization (n_w) for the Polymers Studied

polymer	M_w (kDa)	M_w/M_n	MHS (α)	n_w
$T4_6$	2.2	1.3	0.600	6
$T4_{12}$	4.3	1.1	0.814	12
$T4_{43}$	15	1.7	0.760	43
$A4_{42}$	14	1.2	0.643	42

Size and Charge of Polyplexes. Polyplexes were formulated according to our previously published protocol,[11] and the polyplexes formed with linear PEI, $T4_6$, $T4_{12}$, $T4_{43}$, and $A4_{42}$ were examined *via* dynamic light scattering and zeta potential to understand how the differences in polymer chemistry and molecular weight influenced the physical properties of the polyplexes. It was found that polyplexes formulated with $A4_{42}$ and pDNA yielded the smallest nanoparticle size (average diameter = 32.4 ± 0.67 nm) and the highest zeta potential (+35.1 ± 5.9 mV) (Figure 1). Despite

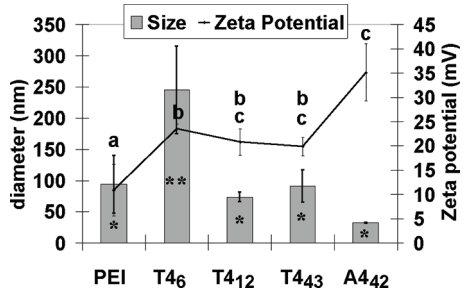

Figure 1. Size and zeta potential measurements for polyplexes formed with linear PEI, $T4_6$, $T4_{12}$, $T4_{43}$, and $A4_{42}$. PEI polyplexes were formed at an N/P ratio of 5, and the T4 and $A4_{42}$ polyplexes were formed at an N/P ratio of 20. Different asterisks on size measurement bars denote statistical significance ($p < 0.05$) according to the Tukey–Kramer HSD method ($n = 3$). The zeta potential measurements for $A4_{42}$ were also found to be statistically significant from that of the other polymers using the same method, where measurements denoted by different letters are statistically significant from each other.

changing the molecular weight, there was no significant difference in zeta potential values when comparing the three T4 analogues; however, the shorter polymer, $T4_6$, formed much larger polyplexes (about 250 nm) than the longer vehicle analogues $T4_{12}$ and $T4_{43}$, which were around 80 nm (Figure 1). Polyplexes formed with linear PEI were similar in size to $T4_{12}$ and $T4_{43}$, but the zeta potential was lower, and this is likely due to the fact that PEI polyplexes were formed at an N/P ratio of 5 rather than 20, as recommended by the manufacturer for transfection.

Protein Expression. To study how polymer molecular weight and structure affect the degree of protein expression, HeLa cells were transfected with polyplexes formed with each of the five different polymers and luciferase expression was measured after 48 h by quantifying relative light units (RLU) per milligram of protein; all RLU was normalized to the cells only control (Figure 2). JetPEI at an N/P ratio of 5 along with $T4_{43}$ and $A4_{42}$ at N/P ratios of 20 yielded similarly higher luciferase expression compared to the lower molecular weight polymers $T4_6$ and $T4_{12}$. Interestingly, the luciferase expression of polyplexes created with pDNA and the T4 derivatives increase with increasing molecular weight by 4 orders of magnitude going from $T4_6$ to $T4_{43}$.

Induction of Apoptosis. Cationic polymers utilized for the delivery of polynucleotides may elicit toxicity that results in apoptosis in a number of ways. Previous studies implicate that both 25 kDa branched[8,9] and 750 kDa linear[8] PEI have two distinct toxicity pathways: one exhibited early in transfection and another occurring after DNA release from the polymer–DNA complex (polyplex) several hours after transfection. The current study focuses on several potential mechanisms of toxicity in order to understand how the polymer structure affects the cytotoxic pathways of these gene delivery vehicles. There are several possible sites for apoptosis initiation during transfection (Figure 3). The effect of polymer structure (with

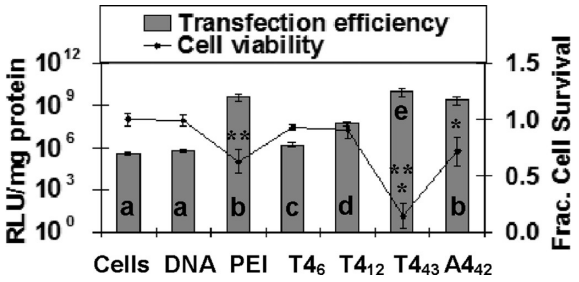

Figure 2. Luciferase gene expression results of polyplexes formulated with pDNA and each of the five different polymers in HeLa cells. Luciferase expression was measured 48 h after transfection; all data are normalized to the cells only control. Cells were transfected with JetPEI (PEI) at an N/P ratio of 5. All other polymers were used at an N/P ratio of 20. Statistical analysis for expression efficiency was performed using the Tukey–Kramer HSD method on the log of the data (n = 6). Bars with different letters are statistically significant from each other (p < 0.05). For the cell viability data, T4$_{43}$ is significantly lower than A4$_{42}$ and PEI (p < 0.05, denoted with similar asterisks), and PEI, T4$_{43}$ and A4$_{42}$ were all statistically significant from the cells only and DNA only controls (p < 0.05) according to the Tukey–Kramer HSD method (n = 6).

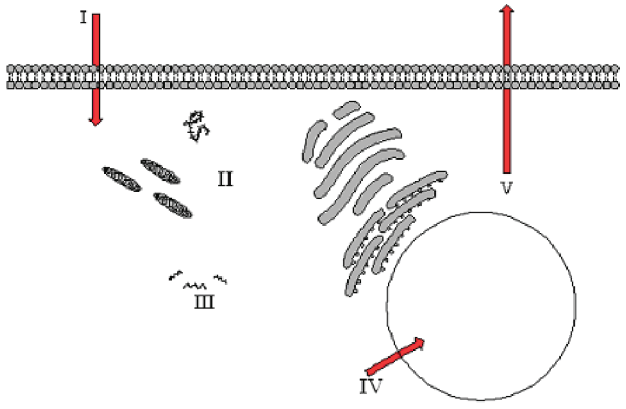

Figure 3. Possible routes of polymer/polyplex cytotoxicity: (I) cellular entry *via* direct membrane permeabilization, (II) interaction with organelles or proteins during intracellular trafficking, (III) harmful products formed upon polymer degradation, (IV) nuclear entry *via* nuclear envelope permeabilization, and (V) cellular exit.

or without hydroxyls in the backbone) and molecular weight on several potential mechanisms of cytotoxicity were tested in the current study. These include plasma membrane permeabililzation (Figure 3, I), the effects of reactive oxygen species (ROS) (Figure 3, III), and the mechanism of how polymer–DNA complexes (polyplexes) enter the nucleus (Figure 3, IV).

Changes in mitochondrial membrane potential as well as phosphatidylserine exposure (markers of apoptosis) were initially used to gauge the timing of apoptosis initiation. All polymers were able to depolarize mitochondrial membrane potential as evidenced by a decrease in DiIC(1)5 fluorescence (Figure 4a) as well as induce phosphatidylserine exposure as evidenced by an increase in Annexin V–FITC fluorescence (Figure 4b) within 30 min after transfection (Figure 4). There was no statistically significant difference in the amount of mitochondrial membrane potential reduction or the amount of phosphatidylserine increase between the T4 polymers and the structures lacking hydroxyl groups (A4$_{42}$ and linear PEI polymers) at this early time point. However, four hours after transfection, a dramatic difference in apoptotic signals was

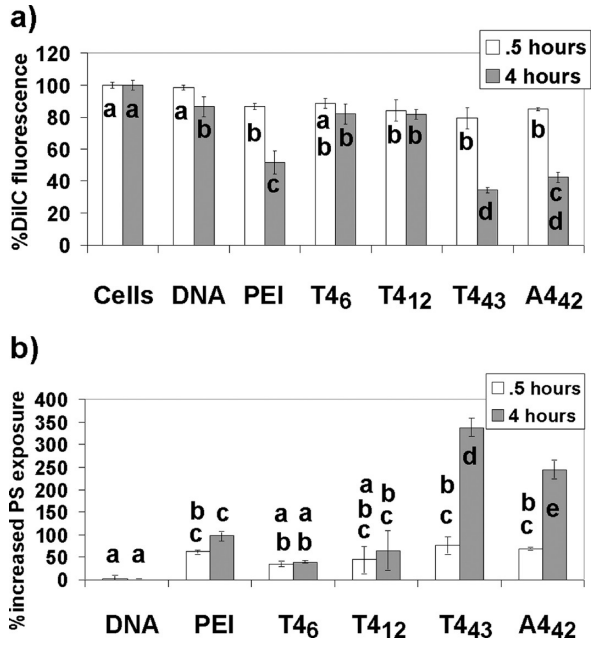

Figure 4. (a) Mitochondrial membrane potential measured by DiIC(1)5 fluorescence normalized to the cells only control and (b) phosphatidylserine (PS) exposure measured by Annexin V binding assay in HeLa cells transfected with polyplexes formed using PEI, T4, and A4$_{42}$. The data in (b) is presented as the percent increase in PS exposure compared to the cells only control. Letters represent statistical analysis; bars with different letters are statistically significant (p < 0.05) according to the Tukey–Kramer HSD method (n = 3).

found. Polyplexes formed with linear PEI, T4$_{43}$, and A4$_{42}$, the longest polymers, reduced mitochondrial membrane potential to a greater extent when compared to the data from T4$_6$ and T4$_{12}$. This result indicates that the longer polymers induce apoptosis and lead to cell death faster than shorter structures. Interestingly, polyplexes formed with the carbohydrate-containing T4$_{43}$ induced the most phosphatidylserine exposure and mitochondrial membrane depolarization, indicating that the hydroxyls in the T4$_{43}$ backbone could contribute to toxicity at longer degrees of polymerization. Both T4$_{43}$ and A4$_{42}$ induced significantly more phosphatidylserine exposure than PEI and T4$_{12}$ 4 h after transfection (Figure 4b). These data agree with the lower viability data observed for T4$_{43}$ in the previous transfection experiment (Figure 2). It is interesting to note that the polymer structures responsible for inducing apoptotic signals (Figure 4) are the same structures with the highest extent of luciferase expression (Figure 2).

Plasma Membrane Interactions. The plasma membrane is the first barrier polyplexes encounter during transfection, and prior studies have indicated that cationic polymers are able to disrupt and induce pore formation in the plasma membrane of cells.[19–21] Previous research on these systems completed by our group has shown that polyplexes formed with JetPEI and T4 enter the cell in different ways, and this could cause different interactions leading to or preventing toxicity.[14] Also of significance, previous work by other groups has shown that direct permeabilization of the plasma membrane is observed by branched and linear PEI, and this permeabilization is implicated as a potential mechanism of cytotoxicity.[1,9,22] It is possible that the different cytotoxic profiles observed for linear PEI vs the PGAAs are a result of their different mechanisms of cellular entry.[14]

dx.doi.org/10.1021/mp200368p | *Mol. Pharmaceutics* 2012, 9, 523–538

To further support previous studies showing that the T4 polymers and PEI enter the cell *via* different routes,[14] cells were transfected in the presence or absence of EGTA, an extracellular calcium chelator. EGTA has been shown to disrupt cell−cell junctions and expose basolateral surfaces of endothelial cells,[23] which can result in increased cellular binding and transfection efficiency of several nonviral DNA delivery vehicles.[23−25] We found that chelating extracellular calcium resulted in an increase in cellular internalization for polyplexes formed with linear PEI two hours after transfection. Conversely, the removal of extracellular calcium with EGTA had a slight inhibitory effect on the internalization of $T4_{12}$ and $T4_{43}$ polyplexes, and did not have an effect on the uptake of $A4_{42}$ polyplexes (Figure 5).

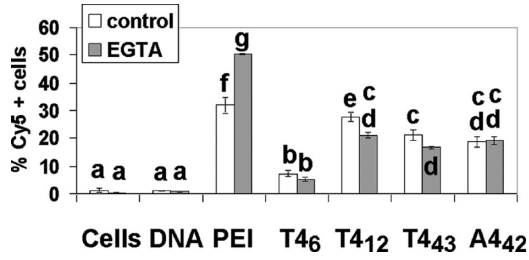

Figure 5. The effect of EGTA, an extracellular calcium chelator, on cellular uptake of polyplexes formed with and the indicated polymers and Cy5-pDNA 2 h after transfection. Bars represent the mean ± standard deviation. Bars with different letters are statistically significant from each other ($p < 0.05$) according to the Tukey−Kramer HSD method ($n = 3$).

To further study how polymer length and structure influence the interaction of polyplexes with the plasma membrane and the mechanism of cellular uptake, confocal microscopy was used to monitor colocalization of polyplexes and the plasma membrane 30 min after transfection. AlexaFluor-488-conjugated wheat germ agglutinin, a lectin that binds to *N*-acetylglucosamine and sialic acid residues,[26,27] was used to label the plasma membrane. The software ImageJ[17] was used to calculate Manders coefficients for polyplexes formed with Cy5-labeled pDNA and the wheat germ agglutinin on the plasma membrane as a measure of colocalization.[28,29]

Z-stacks of HeLa cells were taken using slice thicknesses of 0.39 μM/slice, and colocalization was analyzed throughout the entire stack. The images shown in Figure 6 represent one slice of the z-stack. Based on the confocal images and Manders coefficients (Figure 6), we conclude that all polyplexes have some interaction with the plasma membrane as early as 30 min after transfection, and the data reveals that $T4_{12}$, $T4_{43}$, $A4_{42}$, and PEI all have a similar degree of interaction with the cell membrane. It was noticed that polymer $T4_6$ had the lowest interaction with cells and internalization when compared with the other polymers (Figure 6), and these results correlate with the previous observation that $T4_6$ has the lowest luciferase expression efficiency. Polyplexes formed with the other polymers exhibit significant polyplex internalization. Several internalized polyplexes are denoted by the white arrows in Figure 6, with polyplexes for PEI (Figure 6b), $T4_{12}$ (Figure 6d), $T4_{43}$ (Figure 6e), and $A4_{42}$ (Figure 6f) all illustrating more polyplex internalization than $T4_6$ (Figure 6c). To determine whether there was a difference in plasma membrane permeability at this time point, a propidium iodide exclusion assay was performed.

Plasma Membrane Permeability. Propidium iodide (PI) is a small molecule that has a diameter of ∼1 nm[30] and is normally excluded from cells with an intact plasma membrane but can penetrate cells in which the plasma membrane has been disrupted (and is also commonly used as a marker of dead cells). PI fluorescence was used as a measure of plasma membrane permeability at 30 min and 4 h after transfection. It is apparent that $T4_{43}$ induces the most membrane disruption 4 h after transfection and is interesting to note that the polymers with the highest expression efficiency are also the structures inducing the most plasma membrane permeability according to these PI assays (Figure 7). As observed in the mitochondrial membrane potential and phosphatidylserine exposure assays (Figure 4), there is no significant difference in the degree of membrane permeability induced by the polyplexes 30 min after transfection, the time point where polyplexes were shown to interact with the plasma membrane (Figure 6). However, 4 h after transfection, we see a dramatic increase in membrane permeability in cells treated with linear PEI, $T4_{43}$, and $A4_{42}$ compared to the cells only control. Indeed, it is evident that the three polymers with the highest expression efficiency are able to induce the most plasma membrane damage. Prevette et al. have shown that an increase in plasma membrane permeability does not increase expression efficiency,[30] but perhaps if these polymers are able to induce plasma membrane permeability, they are able to induce membrane permeability in other organelles, including the nucleus. Based on these studies, it is difficult to tell whether the plasma membrane permeability is induced directly by the polymers, or is a consequence of apoptosis activation at this time point; we observe an increase in PI fluorescence (Figure 7), a decrease in mitochondrial membrane potential (Figure 4a), and an increase in phosphatidylserine exposure (Figure 4b) within 30 min of transfection. We do notice a trend in both the apoptosis studies (Figure 4) and the PI study (Figure 7). It seems that in each of the different assays, 30 min after transfection there are no dramatic differences between the polymers, and $T4_{42}$ and $A4_{43}$ are the only polymers statistically significant from the DNA only control at this time point. However, 4 h after transfection, cells transfected with PEI, $T4_{43}$, and $A4_{42}$ exhibit significantly more mitochondrial depolarization (Figure 4a), phosphatidylserine exposure (Figure 4b), and PI fluorescence (Figure 7) when compared to $T4_6$ and $T4_{12}$. Furthermore, it appears that $T4_{43}$ induces the most cellular disruption based on these studies when compared to the other polymers. Based on the dramatic changes in toxicity profiles between the polymers 4 h after transfection, it was of interest to us to perform further studies at this time point to determine the cause of apoptosis initiation.

Toxicity of Potential Polymer Degradation Products. It has been previously shown in several previous studies in the field of nucleic acid delivery that the molecular weight of polymeric delivery vehicles influences their cytotoxicity profile to a large degree; higher molecular weight polymers generally induce more toxic effects and cell death.[6,31−34] Based on previous studies in our group, one main difference between the T4 structures examined herein as compared to polymers $A4_{42}$ and linear PEI is that the T4 polymers (and our class of PGAAs) are degradable.[16] It is possible that the T4 structures degrade into lower molecular weight polymers or byproduct that may or may not affect the cell viability. However, the mechanism of polymer degradation once in cells is not currently understood.

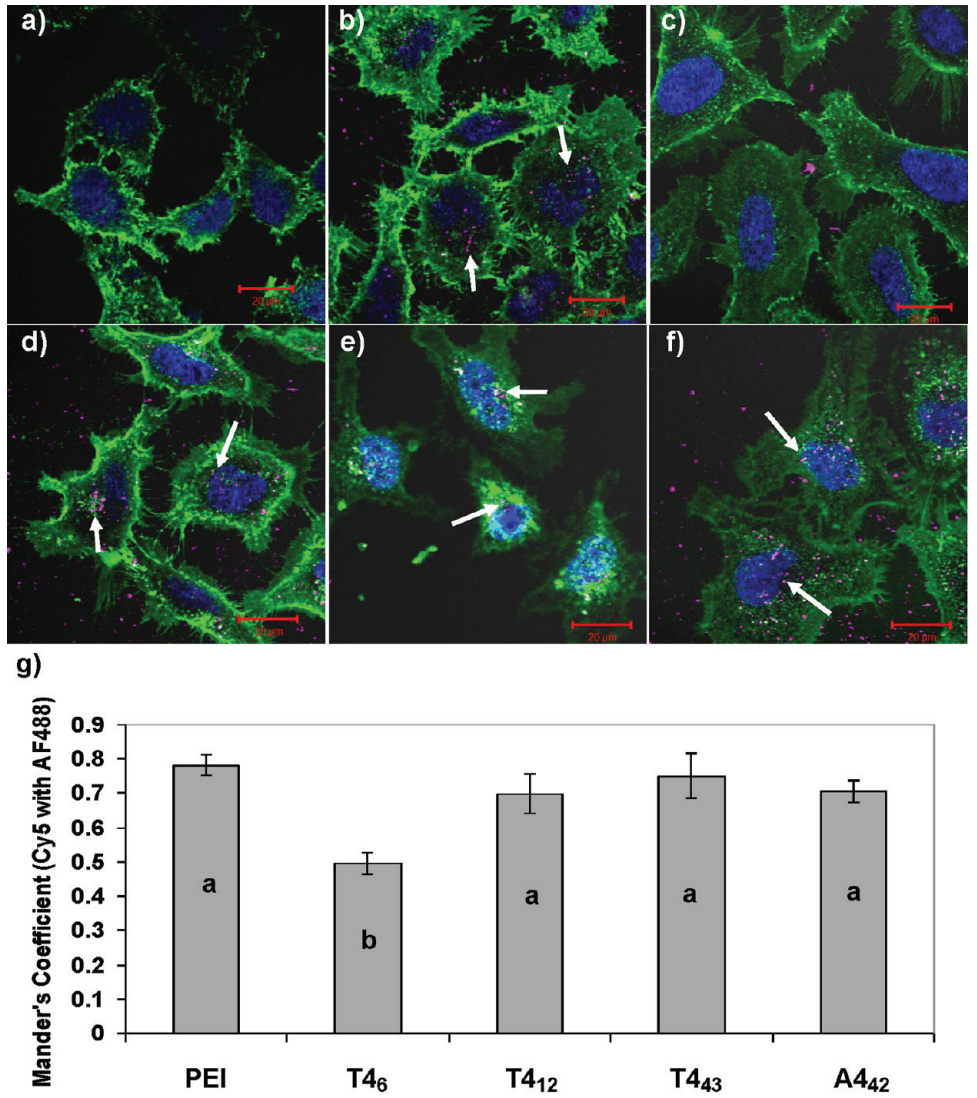

Figure 6. Confocal microscopy images of HeLa cells 30 min after being transfected with polyplexes formed with Cy5-labeled pDNA and the following polymers: (a) pDNA only; (b) JetPEI (PEI); (c) $T4_6$; (d) $T4_{12}$; (e) $T4_{43}$; (f) $A4_{42}$. Colors represent the following: green = WGA AF488-labeled cytosol; blue = DAPI-labeled nucleus; magenta = Cy5-labeled pDNA. Scale bar = 20 μm. Arrows denote sites of polyplex internalization. (g) Manders coefficients between each polyplex type (formed with Cy5-pDNA) and AlexaFluor-488-conjugated wheat germ agglutinin-labeled plasma membrane. Bars with different letters are statistically significant from each other ($p < 0.05$) according to the Tukey–Kramer HSD method ($n = 3$).

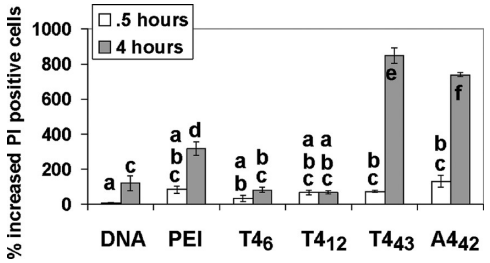

Figure 7. Measurement of propidium iodide fluorescence in HeLa cells after transfection with each polyplex type at time points of 30 min and 4 h as measured *via* flow cytometry. Data are presented as the percent increase in PI positive cells as normalized to the cells only control.

To further examine the role of degradation product toxicity in the T4 polymer series, the toxicity of L-tartaric acid and pentaethylenehexamine hexahydrochloride (N6), the monomers used to synthesize the T4 polymers and suspected degradation byproduct, was examined *via* MTT assay. The cells were treated for 4 and 24 h with the L-tartaric acid and N6 at concentrations of 100 μg/mL. We saw no significant cytotoxic responses induced in the cells at either of these time points (Figure 8).

It is possible that, once in the cell, the polymers are catabolized by other means besides hydrolysis and the higher molecular weight polymers create higher oxidative stress over time; however, studies to examine this effect are beyond the scope of the current manuscript. Based on these data, the polymers that are shorter in length are certainly less toxic than the same structures that are longer in length. Furthermore, the individual components of the T4 polymers (L-tartaric acid and N6) do not elicit any cytotoxic responses within 4 h (Figure 8), so the apoptotic signals elicited by the polyplexes at this time point (Figure 4) are most likely not a result of polymer degradation products.

Nuclear Membrane Permeabilization. These polymer gene delivery vehicles are able to deliver pDNA to the nucleus

dx.doi.org/10.1021/mp200368p | *Mol. Pharmaceutics* 2012, 9, 523–538

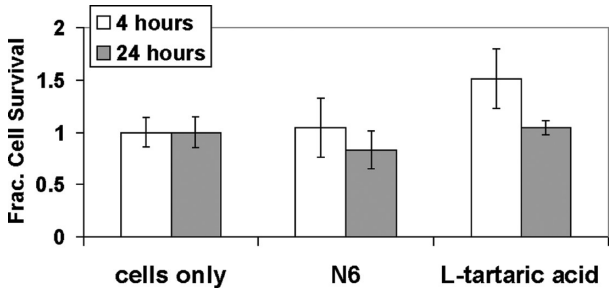

Figure 8. Toxicity of the components of the T4 polymers as measured by MTT assay. Cells were treated with either N6 or L-tartaric acid at a concentration of 100 μg/mL for the indicated time points. These data from the monomer treatments were not statistically significant from the data for the cells only control as determined by the Tukey–Kramer HSD method (n = 3).

of their target cells, but the mechanism as to how the pDNA from the polyplex is transported across the nuclear membrane for transcription is currently unknown. While previous studies indicate that polyplexes are able to induce plasma membrane damage that contributes to cytoxicity, we were interested to examine the role of nuclear membrane damage in the increase of protein expression efficiency, toxicity, and cell death. The nuclear membrane, being a double bilayer membrane, is more resistant to permeabilization than the plasma membrane. However, it is unknown if polyplexes could potentially disrupt the nuclear membrane as a mechanism of nuclear entry. Prior studies indicate that polyplexes are able to deliver their DNA cargo into the nucleus when the nuclear envelope degrades in preparation for cell division.[35−38] This is a likely mechanism, as higher protein expression is often observed in rapidly dividing cells. However, this hypothesis does not explain transfection in nondividing or slowly dividing cells. For example, Brunner et al. have shown that the amount of protein expression in cells transfected with linear PEI is not affected by cell cycle.[39] It is interesting to note that, in those studies, branched PEI exhibits more cell cycle dependence than linear PEI as well as exhibiting lower protein expression;[35,39] this indicates that efficient means of nuclear delivery other than nuclear envelope breakdown during mitosis improve polymer expression efficiency. Other studies show that, in order to deliver the plasmid DNA into the nucleus, intracellular nuclear import machinery must be utilized.[38,40,41] The mechanisms as to how polyplexes are able to utilize this remain blurred, but research shows that the sequence of the plasmid DNA plays a role. Certain DNA sequences are able to bind to transcription factors. The incorporation of sequences to bind to transcription factors, such as Nf-κB,[42−44] has been used as a strategy to increase transfection efficiency. Once bound to the transcription factors, plasmid DNA is able to achieve nuclear entry *via* the nuclear pore complexes (NPCs).[45,46] Another strategy to increase nuclear entry is to use nuclear localization signals.[47] Direct nuclear permeabilization by polyplexes, however, is a mechanism of nuclear entry that has not been thoroughly studied. It should be noted here that the polymers used in the current study do not contain a known nuclear localization signal. Also, the plasmid DNA used in this study contains a CMV promoter, and previous work has shown that plasmids with this promoter are not actively trafficked by the cell to the nucleus when injected into the cytosol of smooth muscle cells.[48−50] Given that the polymers with the highest expression efficiency (Figure 2) also induce the most plasma membrane permeability (Figure 7), it was of interest to us to determine whether the studied polyplexes deliver pDNA to the nucleus *via* direct nuclear permeabilization; thus yielding a mechanism for possible cytotoxicity and polymer-based DNA nuclear delivery other than nuclear envelope breakdown during mitosis. To examine this, polyplexes were formed with Cy5-labeled plasmid DNA, and HeLa cells were transfected with each polyplex type for 4 h, the time point at which the differences in the induced apoptotic signals were apparent (Figure 4). After 4 h, the nuclei from the transfected cells were removed, and Cy5 fluorescence and PI fluorescence were measured using flow cytometry (Figure 9). Nuclear isolation was confirmed using microscopy

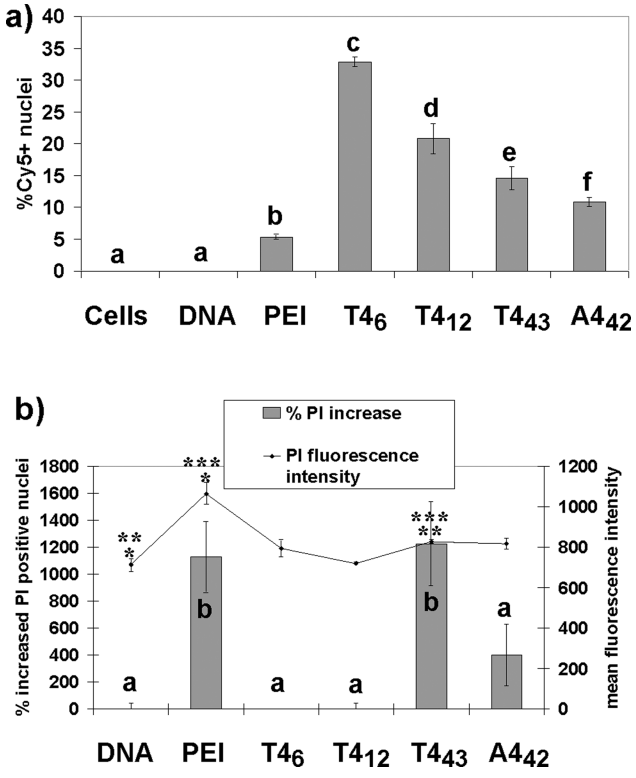

Figure 9. Nuclei were isolated from cells transfected with the indicated polymers 4 h after transfection and analyzed using flow cytometry. (a) Nuclear association between polyplexes and nuclei measured by Cy5 fluorescence and (b) nuclear membrane permeability induced by polyplexes, which is shown as the percent increase in propidium iodide (PI) positive nuclei (bars) and PI fluorescence intensity (line) as compared to the cells only control. Bars with different letters represent means that are statistically significant from each other (p < 0.05) as determined by the Tukey–Kramer HSD method (n = 3). For fluorescence intensity, points with matching asterisks represent means that are statistically significant (p < 0.05) from each other determined by the Tukey–Kramer HSD method (n = 3).

(not shown) and static light scattering (Figure S4 in the Supporting Information). It should be mentioned here that, using this flow cytometric method, we were unable to determine whether the Cy5-labeled plasmid DNA was actually inside the nucleus or attached to the nuclear membrane; it is likely a combination of both, and we arbitrarily name this "nuclear association". We observed an astounding trend: polymer length does seem to affect nuclear interactions, and when considering polymer molecular weight, the shorter the polymer, the higher the pDNA association with the nucleus. The nuclei from T4$_6$-treated cells had higher Cy5 fluorescence

dx.doi.org/10.1021/mp200368p | *Mol. Pharmaceutics* 2012, 9, 523−538

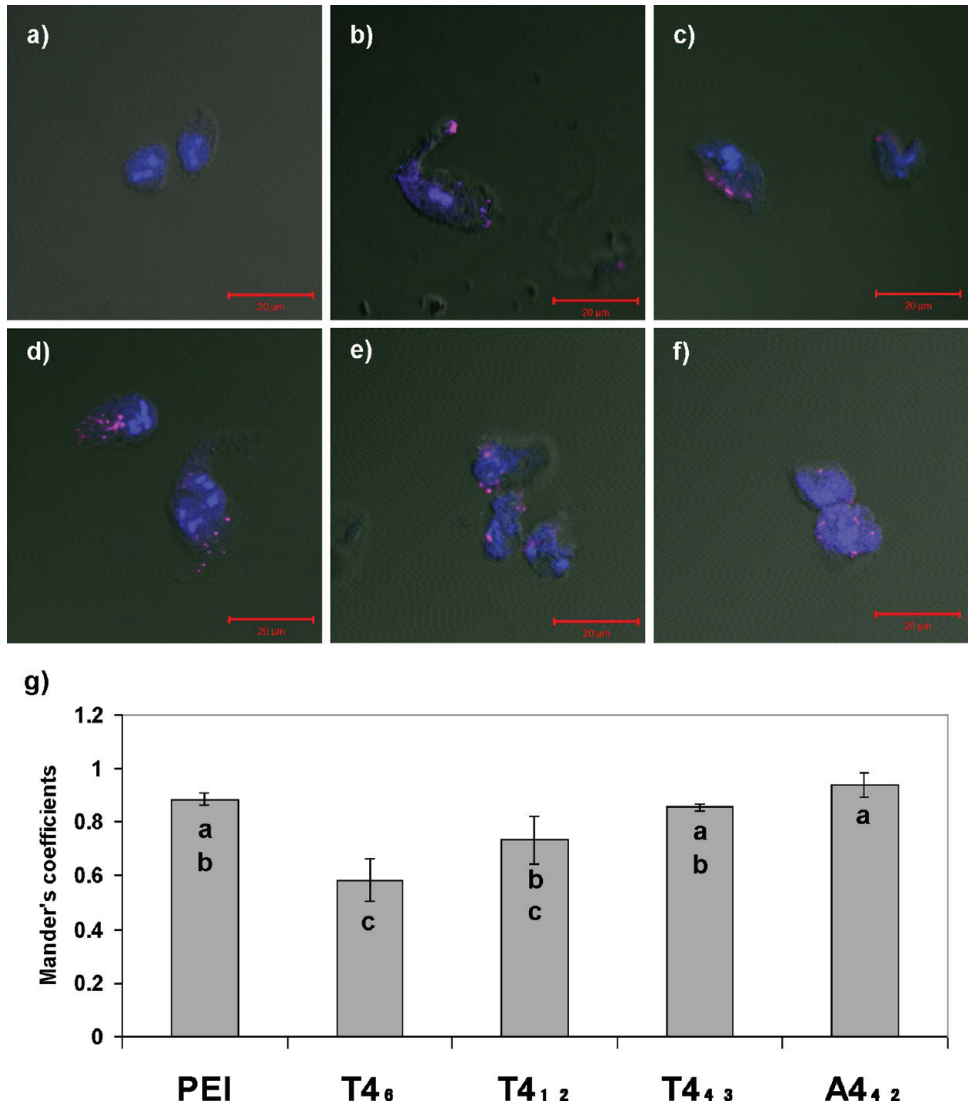

Figure 10. Nuclei isolated from cells transfected with the following: (a) pDNA only; (b) JetPEI (PEI); (c) $T4_6$; (d) $T4_{12}$; (e) $T4_{43}$; (f) $A4_{42}$. Colors represent the following: blue = propidium iodide-labeled nucleus; magenta = Cy5-labeled pDNA. Scale bar = 20 μm. (g) Manders coefficients between Cy5-labeled pDNA and propidium iodide to signify pDNA nuclear import. Bars with different letters represent means that are statistically significant ($p < 0.05$) as determined by the Tukey–Kramer HSD method ($n = 3$).

than polyplexes formed with higher molecular weight polymers (Figure 9a), indicating greater association of $T4_6$ polyplexes with the nucleus than other polyplexes. The nuclei from cells transfected with polyplexes formed with the higher molecular weight polymers PEI, $T4_{43}$, and $A4_{42}$ show an increase in propidium iodide fluorescence, indicating an increase in nuclear membrane permeability (Figure 9b). These trends are interesting, because although pDNA delivered with $T4_6$ displayed higher nuclear association, it also has the lowest expression efficiency of the polyplexes tested. Also, the higher molecular weight polymers PEI, $T4_{43}$, and $A4_{42}$ display lower nuclear association than $T4_6$, but higher expression efficiency. This higher expression efficiency also correlates with increased PI fluorescence in whole cells (Figure 7) and isolated nuclei in the cases of PEI and $T4_{43}$ (Figure 9b).

It was our hypothesis that although $T4_6$ was able to get pDNA to the nuclear membrane, it was unable to enter the nucleus since $T4_6$ polyplexes did not induce as much membrane permeability as the polymers with higher expression efficiency (Figure 7). It is likely that the increased Cy5 fluorescence observed in $T4_6$-transfected nuclei was due to polyplexes binding to the nuclear surface. In order to determine this, the nuclei from the isolated cells used for the flow cytometry experiments were fixed and deposited onto coverslips, and they were then imaged using confocal microscopy. The confocal microscopy results supported our hypothesis; $T4_6$ polyplexes were found on the periphery of the nuclear membranes, while polyplexes formed with linear PEI, $T4_{43}$ and $A4_{42}$ were found inside the nuclei (Figure 10). Polyplexes formed with $T4_{12}$ were found both on the periphery of the nuclei and inside of the nuclei, but to a lesser extent than polyplexes formed with the higher molecular weight polymers. To further confirm this, z-stacks of each image were taken and fluorescence was quantified for each slice using the software ImageJ (Figure S5 in the Supporting Information). Indeed, $T4_6$-treated nuclei exhibited higher Cy5 fluorescence near the surface of the nuclei, while PEI, $T4_{43}$ and $A4_{42}$-treated nuclei exhibited Cy5 fluorescence from the inside of the nuclei. Furthermore, Manders coefficients were measured to observe colocalization with Cy5-labeled pDNA and propidium iodide in

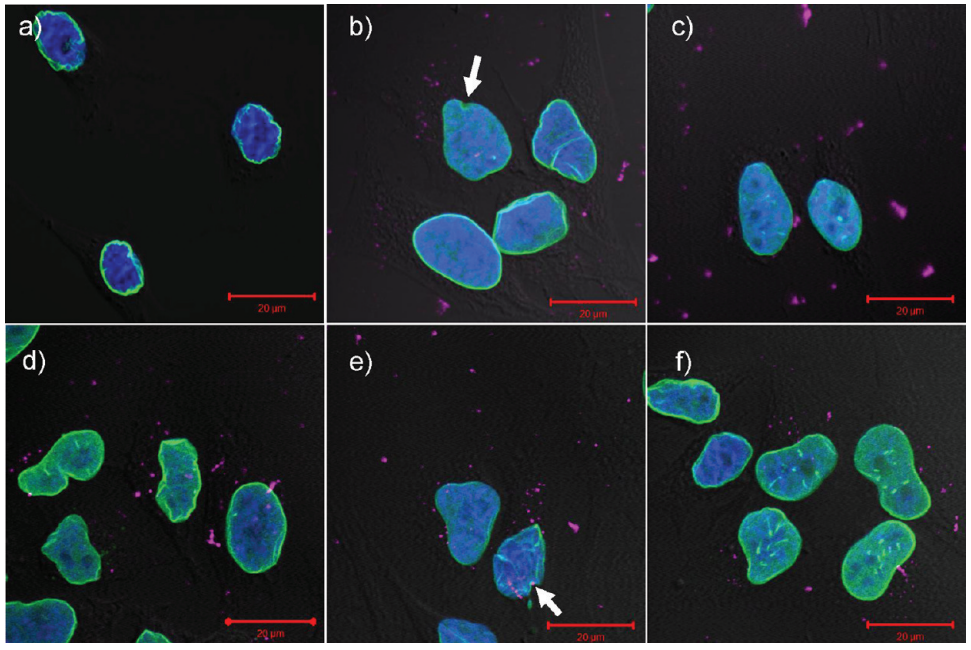

Figure 11. Confocal images of HeLa cells fixed 4 h after transfection. Cells were transfected with the following: (a) DNA only; (b) JetPEI (PEI); (c) $T4_6$; (d) $T4_{12}$; (e) $T4_{43}$; (f) $A4_{42}$. Colors represent the following: blue = nucleus; green = nuclear lamin; magenta = pDNA. Scale bar = 20 μm. White arrows indicate sites of deep nuclear envelope indentation.

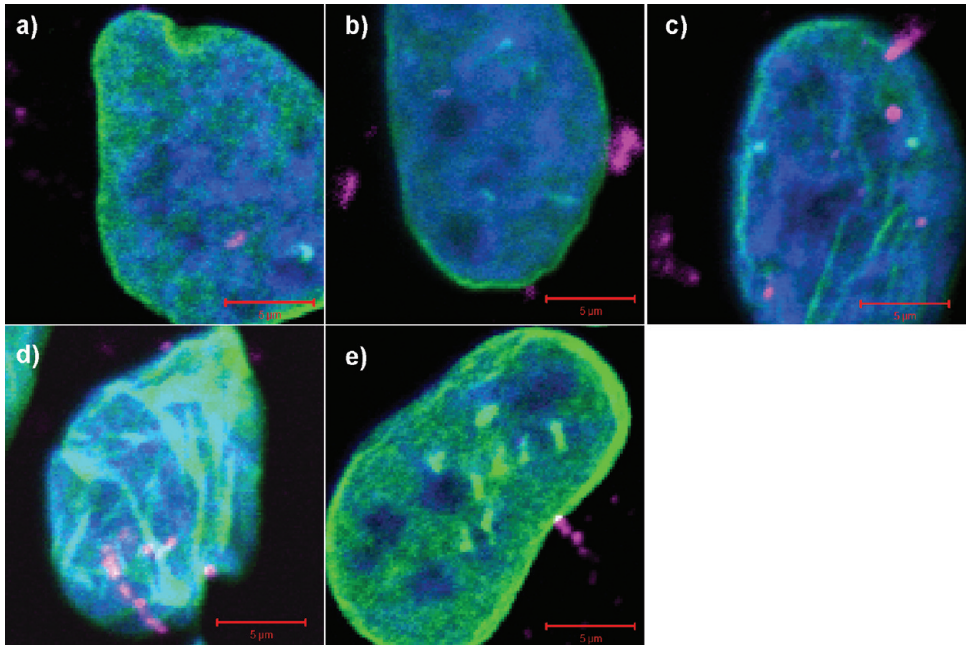

Figure 12. Confocal microscopy images of the nuclei in whole HeLa cells transfected with polyplexes formed with Cy5-pDNA and (a) JetPEI (PEI); (b) $T4_6$; (c) $T4_{12}$; (d) $T4_{43}$; (e) $A4_{42}$. The nucleus is shown as blue, nuclear lamin is shown as green, and the polyplexes are shown as magenta. Scale bar = 5 μm.

the nucleus to verify which polymers were able to induce nuclear import of the pDNA. The trends observed with expression efficiency (Figure 2), plasma membrane disruption (Figure 7), and nuclear membrane permeability (Figure 9b) were also evident when studying nuclear pDNA import; the polymers with the highest expression efficiency exhibited the most colocalization between pDNA and propidium iodide, with PEI, $T4_{43}$ and $A4_{42}$ exhibiting significantly more colocalization than $T4_6$ (Figure 10g).

However, the increased PI fluoresce in isolated nuclei observed in Figure 9 could also be a result of apoptosis initiation in the cells; we have already shown that the polymers with the highest expression efficiency also induce apoptosis at this time point (Figure 4), and it is possible that the polymers' ability to induce apoptosis disrupts the nuclear envelope. To further study this, we first wanted to determine if the polyplexes were in the vicinity of the nuclei at this time point.

Nuclear Interactions. The flow cytometry results indicated that $T4_6$ had higher nuclear association than the other polymers

4 h after transfection, and the degree of nuclear association decreased with an increase in polymer length (Figure 9a). To confirm that polyplexes were in fact reaching the nuclear membrane 4 h after transfection, HeLa cells were transfected as described above for 4 h, and then the cells were fixed in 4% paraformaldehyde, immunostained to label the nuclear lamin, and imaged using confocal microscopy. Images of the whole cells with the DiC images are shown in Figure 11, illustrating that all polyplexes are able to enter the cells and reach the nucleus 4 h after transfection. The nuclei of the transfected cells are the focus of the confocal images shown in Figure 12 to further illustrate nuclear membrane ruffling and colocalization of the polyplexes with the nuclear lamin.

Nuclear envelope ruffling was evident in all nuclei to some extent, but we observed deeper invaginations in the nuclear envelope in cells treated with JetPEI (Figure 11a) and $T4_{43}$ (Figure 11e) as indicated by the white arrows. It is possible that the observed nuclear envelope ruffling is a result of apoptosis, but the image for $T4_{43}$ is especially striking. In the case of $T4_{43}$, there is evidence of nuclear membrane disruption at the site of polyplex contact (Figure 12d). Manders coefficients were calculated to determine colocalization between the polyplexes and the nuclear lamin using the software ImageJ. Z-stacks of each image were taken using overlapping slices of 0.39 μm, and Manders coefficients were calculated using the entire z-stack. We observed slight differences in the degree of colocalization between the different polymers, these results confirm that the polyplexes were reaching the nuclear envelope by 4 h (Figure 13). Our results indicate that polyplexes formed with $T4_{43}$ had higher colocalization with the nuclear lamin 4 h after transfection compared to PEI, $T4_{12}$, and $A4_{42}$ and had similar colocalization compared to $T4_6$. Polyplexes formed with $T4_6$, despite having lower expression efficiency than PEI, displayed higher colocalization with the nuclear lamin, and these results support the flow cytometry data. Because $T4_6$ is able to reach the nucleus to the same extent as the polymers displaying higher expression efficiency, we conclude that reaching the nucleus is not the limiting factor for successful protein expression with the polymers tested; effective nuclear import of pDNA is also necessary, and we show that the degree of pDNA nuclear import is influenced by polymer structure. As seen in Figure 10g, $T4_6$ has the lowest incidence of colocalization between pDNA and propidium iodide, indicating lower nuclear import. The trends between nuclear interactions and nuclear envelope permeability (Figure 9), colocalization with the inner nucleus (Figure 10g), and transfection efficiency (Figure 2) are apparent. However, it is still unclear whether the polyplexes are directly permeabilizing the nuclear envelope or if the increased nuclear permeability is a result of apoptosis initiation. To test whether polyplexes alone could induce nuclear envelope permeability, studies on isolated nuclei were conducted.

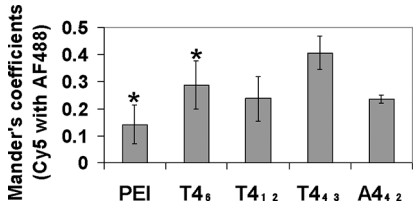

Figure 13. Manders coefficients for the colocalization of each polyplex type (formed with Cy5-pDNA) with nuclear lamin antibody (labeled with AF488) for confocal microscopy images taken of cells transfected with polyplexes for 4 h. Measurements with similar asterisks above them were found to be statistically significant ($p < 0.05$) as determined by the Tukey–Kramer HSD method ($n = 3$).

Nuclear Envelope Permeability in Isolated Nuclei. As mentioned previously, the increased nuclear envelope permeability observed as increased PI fluorescence (Figure 7) could be a result of apoptosis initiation and not necessarily caused by direct polyplex interaction. To determine whether polyplexes could induce nuclear envelope permeability in a cell-free system, nuclei were isolated from HeLa cells and treated with polyplexes for 4 h. The results are shown in Figure 14.

Trypan blue is a small molecule and is able to diffuse through the nuclear pore complex, so we would expect to see trypan blue staining in all nuclei to some extent, similar to propidium iodide exclusion. However, when observing the isolated nuclei under the microscope, we notice that nuclei treated with PEI (Figure 14c), $T4_{12}$ (Figure 14d), $T4_{43}$ (Figure 14e), and $A4_{42}$ (Figure 14d) all exhibited darker trypan blue staining compared to nuclei treated with pDNA only (Figure 14a) and $T4_6$ (Figure 14b). To further compare these images, image analysis was conducted to calculate the mean pixel intensity of each nuclei present in the images using a particle analysis plugin in the ImageJ software to remove background. We found that nuclei treated with the polymers all exhibited darker fluorescence intensity compared to the nuclei treated with pDNA only (Figure 14g), with PEI, $T4_{43}$ and $A4_{42}$ exhibiting the darkest intensities, indicating that these polymers are able to induce the most trypan blue inclusion (for detailed statistical analysis, see Table S1 in the Supporting Information). Furthermore, we also wanted to test whether inducing apoptosis would increase transfection efficiency due to the aforementioned apoptosis-induced nuclear envelope permeability. With the exception of pDNA only, we saw no increase in expression efficiency in cells treated with 5 μM camptothecin, an apoptosis-inducing agent, compared to control cells (Figure S6 in the Supporting Information).

DISCUSSION

In the current study, we have investigated several potential mechanisms of cytotoxicity for five different polymeric gene delivery vehicles, linear PEI, $T4_6$, $T4_{12}$, $T4_{43}$, and $A4_{42}$. These polymeric delivery vehicles vary in their chemistry (containing or lacking hydroxyls) and molecular weight. The goal of this study was to understand the role of these structural parameters on the biological behavior during pDNA delivery. These behaviors include polyplex size and charge, expression efficiency, potential harmful interactions with the plasma membrane, ability to induce apoptosis, generation of ROS, and whether polyplexes were capable of directly permeabilizing the nuclear membrane. Herein, it was found that the length of the polymer and the composition of the polymer influence cytotoxicity and cell interactions to a large degree.

The first noticeable difference between the polymers was their interactions with pDNA. Based on this data, it appears that the polymer structure plays a role in how plasmid DNA is complexed. The absence of hydroxyls on the $A4_{42}$ polymer seemed to result in a smaller, more positively charged polyplex. However, linear PEI, which also lacks hydroxyl groups, forms polyplexes similar in size to $T4_{12}$ and $T4_{43}$. $T4_6$, however, forms particles double in size compared to all other polymers, indicating that this polymer is unable to compact pDNA into as small a nanoparticle as the other polymers tested. Prior research

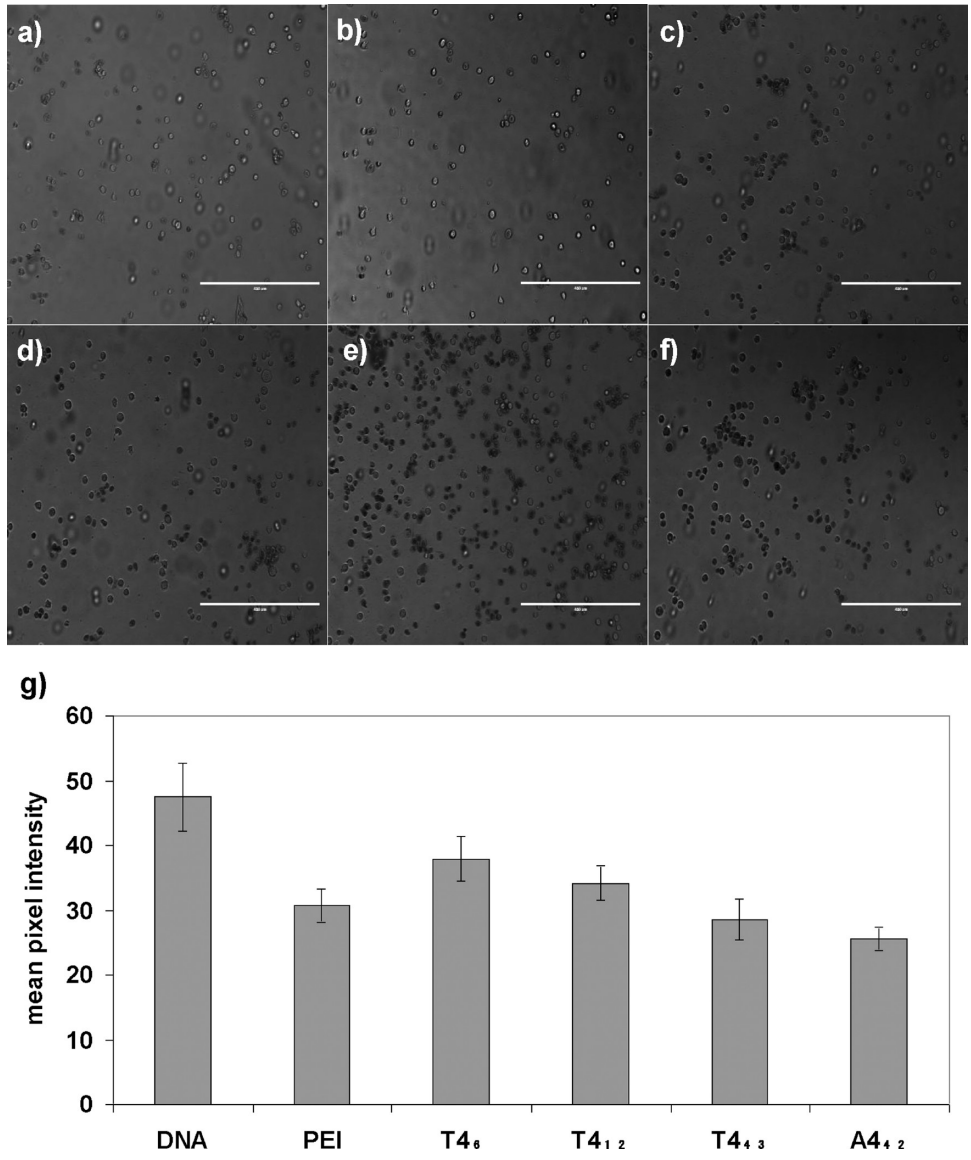

Figure 14. Trypan blue exclusion assay performed on nuclei treated with polyplexes for 4 h. Nuclei were isolated from HeLa cells and treated with (a) pDNA only; (b) JetPEI (PEI); (c) $T4_6$; (d) $T4_{12}$; (e) $T4_{43}$; or (f) $A4_{42}$. Scale bar = 400 μm. (g) Nuclei were counted and analyzed for pixel intensity using ImageJ, and the statistics were calculated using JMP. Roughly 300 nuclei were analyzed for each polyplex, and the Tukey–Kramer HSD test reveal each set of data points to be statistically significant from one another.

in our group has indicated that T4 exhibits significant hydrogen bonding interactions when complexing with plasmid DNA as compared with analogues that do not contain hydroxyl groups.[51,52] The different binding mechanism of T4 vs $A4_{42}$ may account for their difference in polyplex size and charge.[16,51]

In addition, when comparing polymers of similar molecular weight ($T4_{43}$ and $A4_{42}$), we observe that the hydroxyl-containing $T4_{43}$ formed polyplexes of larger size and lower charge (Figure 1), indicating that the hydroxyls do play a role in the complexation of pDNA. We also observed differences in transfection efficiency between these two polymers, with $T4_{43}$ having slightly higher expression efficiency than $A4_{42}$ (Figure 2). Previous work in our group has shown that A4 with a degree of polymerization (DP) of 12 exhibits lower expression efficiency when compared to T4 with a similar molecular weight (DP of 14).[16] This trend is also seen here when studying the expression efficiency of the higher molecular weight derivatives of these polymers. It is likely that the higher expression efficiency of $T4_{43}$ (as compared to $A4_{42}$) results from its ability to degrade, thus providing a mechanism for plasmid DNA release from the polyplex.[16] $T4_{43}$ also exhibits statistically higher luciferase expression than PEI (Figure 2). We were also surprised to find that despite the degradability of $T4_{43}$, it actually appeared to exhibit a statistically significant higher toxicity profile than $A4_{42}$ and PEI, which do not degrade. This led us to hypothesize that, in this case, degradability does not necessarily decrease toxicity. Rather, we propose that the higher toxicity observed with $T4_{43}$ compared to $A4_{42}$ could be a result of $T4_{43}$'s increased induction of nuclear envelope permeability; this would account for not only the increased toxicity of $T4_{43}$ but the higher degree of observed gene expression as well. In fact, when comparing the cytotoxicity of all of the polymers, it was found that high protein expression also correlated with high cytotoxicity and cell death. The cell viability data for polymers $T4_{12}$ and $T4_6$ were not statistically

dx.doi.org/10.1021/mp200368p | *Mol. Pharmaceutics* 2012, 9, 523–538

significant from the cells only and DNA only controls (Figure 2); it appears that the polymers with the highest degree of protein expression (PEI, $T4_{42}$, and $A4_{43}$) exhibited the highest toxicity (Figure 2). To this end, we were interested in the further investigation of the apparent link between expression efficiency and cytotoxicity. Therefore, it is of interest to study the timing and mechanisms of toxicity with these polymeric vehicles, and how the polymer structure influences the cellular mechanisms related to apoptosis.

Previous studies in our group indicate that the hydroxyl groups present in T4 may contribute to pDNA release (*via* hydrolysis) and therefore result in higher expression efficiency than nonhydroxyl containing polymers.[16] To further investigate the role polymer structure has on biological behaviors, we tested the effect of molecular weight and structure on cytotoxicity. Because some of the structures are able to induce apoptosis within 30 min of transfection (Figure 4), it is prudent to study the mechanisms of cellular uptake for these polymers since the cell membrane is the first obstacle to polymer-based gene delivery and could present the first negative interaction leading to toxic effects. We did find that the larger molecular weight polymers were able to induce membrane permeability (Figure 7) and apoptosis (Figure 4) to a larger extent than the smaller molecular weight polymers within 4 h of transfection. The larger molecular weight polymers also had higher interactions with the plasma membrane within 30 min of transfection when compared to the shorter polymers (Figure 6). It is possible that since the higher molecular weight polymers are able to condense plasmid DNA into smaller polyplexes than the lower molecular weight polymers, the mechanism of uptake for the smaller polyplexes will be altered, resulting in different cytotoxic profiles. To further investigate this, intracellular uptake of the polyplexes was studied in the presence of EGTA to determine the role of extracellular calcium. Extracellular calcium is required to maintain membrane fluidity,[53] and without it cells are not able to recover as well after membrane penetration.[54−56] Since cells without extracellular calcium exhibited improved polyplex uptake in the case of PEI, it appears that membrane fluidity could influence PEI transfection. Interestingly, the cells did not exhibit an increase in propidium iodide permeability in the presence of EGTA (Figure S1 in the Supporting Information), thus discounting the idea that membrane permeability, in this case, helps to aid polyplex internalization in the cells. Supporting this observation, a recent study by Prevette et al. indicates that membrane permeability does not play a role in PEI expression efficiency.[30] Collectively considering the current and published results, we hypothesize that a more likely scenario is that the increased basolateral surface of the cells as a result of EGTA treatment could play a role in PEI uptake, and that the different mechanism of cellular uptake plays a role in early cytotoxicity (< 30 min after transfection). EGTA had a slight inhibitory effect on $T4_{12}$ and $T4_{43}$ uptake, further illustrating that the PGAAs are entering the cell *via* different endocytic mechanisms than PEI.[14] It should be noted that the inhibitory effect of EGTA on the uptake of $T4_{12}$ and $T4_{43}$ is similar to results obtained for several lipid−DNA complexes.[57,58] The detailed mechanism as to how decreasing extracellular Ca^{2+} decreases the intracellular uptake of certain gene delivery vehicles while enhancing others remains unknown, but it is speculated that chelation of extracellular calcium could decrease rates of endocytosis.[57,59,60] Collectively, these studies support previous findings that the structure of the polymers influences their endocytic routes.[14] Furthermore, it supports the conclusion that polymer structure influences plasma membrane interactions; the T4 analogues may take a different endocytic route than linear PEI or $A4_{42}$ that involves calcium-mediated endocytosis. The difference in intracellular uptake mechanisms could contribute to the different toxicity profiles for these polymers.

Also, direct plasma membrane permeabilization may be a mechanism of uptake and of cytotoxicity for the larger molecular weight polymers, as evidenced by the increase in plasma membrane permeability. The differences in plasma membrane permeability are apparent as early as 30 min after transfection (Figure 7). There is also a loss of mitochondrial membrane potential at this time point (Figure 4a), indicating that apoptosis has been initiated. An increase in phosphatidylserine externalization was observed within 30 min of transfection for $T4_{43}$ and $A4_{42}$ polyplex-treated cells (Figure 4b), another sign of early apoptosis. However, although some apoptotic responses are evident 30 min after transfection, the time point where colocalization of polyplexes with the plasma membrane is observed (Figure 6), we find that the cytotoxic profiles of the polymers tested become more apparent 4 h after transfection, prompting us to investigate other mechanisms of polymer-induced cytotoxicity.

Previous research in our group has shown that the PGAAs are able to degrade in water and other biologically relevant buffers.[16] Here, we examined if the different cytotoxic profiles exhibited by the polymers tested were a result of T4's ability to degrade into nontoxic byproducts. To this end, we have synthesized different molecular weights of T4 to observe the role that molecular weight plays on T4 toxicity. We do find that the higher molecular weight T4 shows higher cytotoxicity and expression efficiency than its lower molecular weight counterparts, indicating that if T4 does in fact possess the ability to degrade into smaller molecular weight polymers once inside the cell, it could alleviate some of the toxicity observed during polymer-based DNA delivery. We have also tested the toxicity of model T4 degradation products (the monomers) and have found that they do not exhibit cytotoxicity 24 h after treatment at a concentration of 100 μg/mL. It is possible that, depending on the degradation mechanism, there could be toxic byproduct that leads to apoptosis, as is the case with naturally occurring polyamines found in cells.[61−64] Specifically, intracellular catabolism of natural polyamines that are similar in structure to the monomer used to synthesize the T4 structures, such as spermine and spermidine, causes a rise in hydrogen peroxide, leading to oxidative damage and apoptosis initiation.[62] Thus, the degradation products could lead to increased toxicity. Previous studies have revealed that polymer vehicles can elicit oxidative stress; interestingly, cells transfected with chitosan[65] and a PEGylated branched PEI polymer[66] show upregulated oxidative stress genes when compared to 25 kDa branched PEI-treated cells. In the case of the PEGylated branched PEI, the PEGylated polymer induced higher upregulation of more oxidative stress genes than non-PEGylated branched PEI within 6 h of transfection, and it was suggested that this resulted from the higher molecular weight of the PEGylated PEI-based polymers compared to the branched PEI.[66] In light of this previous data, it was of interest to us to study oxidative damage as a potential mechanism of cytotoxicity for the PGAAs. Cells were transfected with the polymers in the presence or absence of aminoguanidine, an inhibitor of several forms of oxidative-induced apoptosis.[67,68] Aminoguanidine was unable to prevent

any cell death from the polyplexes (Figure S2 in the Supporting Information). Furthermore, no increase in reactive oxygen species in PGAA-treated cells was found compared to the cells only control (Figure S3 in the Supporting Information). Taken together, these results reveal that oxidative damage is not a major mechanism of toxicity for the gene delivery polymers tested.

Another potential mechanism of cytotoxicity investigated in the current work is nuclear membrane permeabilization. If the polyplexes are able to induce plasma membrane permeability, then we hypothesized that they may also be able to induce nuclear membrane permeability and thus provide a mechanism of nuclear entry for their plasmid DNA cargo. In addition, the ability to directly permeabilize the nuclear envelope may provide a link between the high toxicity observed with the polymers exhibiting the highest amount of protein expression (Figure 2). We do see polyplex−nucleus interactions 4 h after transfection, the same time point where we observe significant differences in the cytotoxic profiles of the polymers. Our data show increased propidium iodide fluorescence in nuclei isolated from PEI, $T4_{43}$, and $A4_{42}$-treated cells, indicating increased nuclear membrane permeability (Figure 10b). Not only do these three polymers exhibit the most cytotoxic responses four hours after transfection (Figures 4 and 7), but these polymers also have the highest expression efficiency (Figure 2). It is possible that their high transfection efficiency correlates with their ability to permeabilize the plasma membrane, but it is also possible that the induction of apoptosis in cells treated with these polymers induces plasma membrane and nuclear envelope permeability. If this is the case, then these three polymers do not need to wait for nuclear envelope breakdown during mitosis to deliver their plasmid DNA into the nucleus. To determine whether increased membrane permeability (resulting from induction of apoptosis) was the cause of increased expression efficiency with polyplexes formed with the higher molecular weight polymers, cells were transfected in the presence or absence of the apoptosis-inducing agent camptothecin. In the presence of camptothecin, we observed a slight increase in transfection efficiency for cells treated with naked plasmid DNA, but a slight reduction in transfection efficiency for all the polyplex types (Figure S6 in the Supporting Information). This indicates that increased nuclear envelope permeability due to apoptosis is likely not aiding polymer transfection. Furthermore, we also observed increased nuclear permeability to the dye trypan blue in the presence of polyplexes compared to nuclei treated with plasmid DNA only (Figure 14), indicating that the polyplexes are able to induce nuclear envelope permeability in a cell-free system. Further study on the mechanism of nuclear uptake for polyplex-delivered plasma DNA is the focus of ongoing studies in our group.

Overall, we conclude that early cytotoxicity (within 30 min of transfection) could be due, in part, to plasma membrane permeabilization, and that toxicity four hours after transfection, could be due, in part, to nuclear membrane permeabilization. We do notice colocalization between polyplexes and the nuclear envelope at this time point, and polyplexes are able to induce nuclear envelope permeability in isolated nuclei as well as in nuclei isolated from transfected cells. If these polymers are in fact able to permeabilize the nuclear membrane, then it is possible that they are able to permeabilize the membrane of different organelles. Further study on polyplex interaction with other organelles is necessary to make definite conclusions on this matter, since polyplexes are present throughout cells 4 h after transfection (Figure 11) and could potentially interact with a myriad of intracellular processes. Although we predict that nuclear membrane permeabilization may be a mechanism of toxicity, a polymer's ability to permeabilize the nuclear membrane may be desirable for efficient transfection; however, a careful balance between cytotoxicity and high expression efficiency needs to be established. It may be possible to tailor polymers that permeabilize the nuclear envelope to increase pDNA delivery to the nucleus but do not damage the nuclei to such an extent that the cells commit apoptosis.

■ ASSOCIATED CONTENT

Supporting Information

Plasma membrane permeability in the presence of EGTA, cytotoxicity of polyplexes in the presence or absence of aminoguanidine, static light scattering data of whole cells vs isolated nuclei, fluorescence intensity analyzed by z-stack slice, and expression efficiency in the presence or absence of camptothecin. This material is available free of charge via the Internet at http://pubs.acs.org.

■ AUTHOR INFORMATION

Corresponding Author

*Department of Chemistry, University of Minnesota, 207 Pleasant Street SE, Minneapolis, MN 55455. Tel: 612-624-8042. Fax: 612-626-7541. E-mail: treineke@umn.edu.

■ ACKNOWLEDGMENTS

The authors acknowledge Dr. Katye Fichter for helpful discussion in analysis of confocal microscopy images. The authors also acknowledge Marion Ehrich and Stephen Werre for assistance with statistical analyses. Giovanna Grandinetti would like to thank the National Science Foundation MILES IGERT program for financial support. This work was supported by the NIH Director's New Innovator Award Program (1 DP2 OD006669).

■ REFERENCES

(1) Hunter, C. A. Molecular hurdles in polyfectin design and mechanistic background to polycation induced cytotoxicity. *Adv. Drug Delivery Rev.* **2006**, *58*, 1523−1531.

(2) DeSmedt, S. C.; Demeester, J.; Hennink, W. E. Cationic polymer based gene delivery systems. *Pharm. Res.* **2000**, *17*, 113−126.

(3) Vijayanathan, V.; Thomas, T.; Thomas, T. J. DNA nanoparticles and development of DNA delivery vehicles for gene therapy. *Biochemistry* **2002**, *41*, 14085−14094.

(4) Nel, A.; Xia, T.; Madler, L.; Li, N. Toxic potential of materials at the nanolevel. *Science* **2006**, *311*, 622−627.

(5) Boussif, O.; Lezoualc'h, F.; Zanta, M. A.; Mergny, M. D.; Scherman, D.; Demeneix, B.; Behr, J. P. A versatile vector for gene and oligonucleotide transfer into cells in culture and in vivo: polyethylenimine. *Proc. Natl. Acad. Sci. U.S.A.* **1995**, *92*, 7297−7301.

(6) Godbey, W. T.; Wu, K. K.; Mikos, A. G. Size matters: Molecular weight affects the efficiency of poly(ethylenimine) as a gene delivery vehicle. *J. Biomed. Mater. Res.* **1999**, *45*, 268−275.

(7) Bieber, T.; Meissner, W.; Kostin, S.; Niemann, A.; Elsasser, H.-P. Intracellular route and transcriptional competence of polyethylenimine-DNA complexes. *J. Controlled Release* **2002**, *82*, 441−454.

(8) Moghimi, S. M.; Symonds, P.; Murray, J. C.; Hunter, A. C.; Debska, G.; Szewczyk, A. A two-stage poly(ethyleneimine)-mediated cytotoxicity: implications for gene transfer/therapy. *Mol. Ther.* **2005**, *11*, 990−995.

(9) Godbey, W. T.; Wu, K. K.; Mikos, A. G. Poly(ethylenimine)-mediated gene delivery affects endothelial cell function and viability. *Biomaterials* **2001**, *22*, 471−480.
(10) Lv, H.; Zhang, S.; Wang, B.; Cui, S.; Yan, J. Toxicity of cationic lipids and cationic polymers in gene delivery. *J. Controlled Release* **2006**, *114*, 100−109.
(11) Liu, Y.; Wenning, L.; Lynch, M.; Reineke, T. M. Gene delivery with novel poly(L-tartaramidoamine)s. In *Polymeric Drug Delivery I: Particulate Drug Carriers*; Svenson, S., Ed.; American Chemical Society: Washington, DC, 2006.
(12) Lee, C. C.; Liu, Y.; Reineke, T. M. General structure-activity relationship for poly(glycoamidoamine)s: The effect of amine density on cytotoxicity and DNA delivery efficiency. *Bioconjugate Chem.* **2008**, *19*, 428−440.
(13) Liu, Y.; Reineke, T. M. Poly(glycoamidoamine)s for gene delivery: Stability of polyplexes and efficacy with cardiomyoblast cells. *Bioconjugate Chem.* **2006**, *17*, 101−108.
(14) McLendon, P. M.; Fichter, K. M.; Reineke, T. M. Poly-(glycoamidoamine) vehicles promote pDNA uptake through multiple routes and efficient gene expression *via* caveolae-mediated endocytosis. *Mol. Pharmaceutics* **2010**, *7*, 738−750.
(15) McLendon, P. M.; Buckwalter, D. J.; Davis, E. M.; Reineke, T. M. Interaction of poly(glycoamidoamine) DNA delivery vehicles with cell-surface glycosaminoglycans leads to polyplex internalization in a manner not soley dependent on charge. *Mol. Pharmaceutics* **2010**, *7*, 1757−1768.
(16) Liu, Y.; Reineke, T. M. Degradation of poly(glycoamidoamine) DNA delivery vehicles: Polyamide hydrolysis at physiological conditions promotes DNA release. *Biomacromolecules* **2010**, *11*, 316−325.
(17) Rasband, W. S. *ImageJ*; U.S. National Institutes of Health: Bethseda, MA, 1997−2009.
(18) Stevens, M. P. *Polymer Chemistry: An Introduction*, 3rd ed.; Oxford University Press: New York, 1999.
(19) Mecke, A.; Majoros, I. J.; Patri, A. K.; Baker, J. R.; Holl, M. M. B.; Orr, B. G. Lipid bilayer disruption by polycationic polymers: The role of size and chemical functional group. *Langmuir* **2005**, *21*, 10348−10354.
(20) Chen, J.; Hessler, J. A.; Putchakayala, K.; Panama, B. K.; Khan, D. P.; Hong, S.; Mullen, D. G.; DiMaggio, S. C.; Som, A.; Tew, G. N.; Lopatin, A. N.; Baker, J. R.; Holl, M. M. B.; Orr, B. G. Cationic nanoparticles induce nanoscale disruption in living cell plasma membranes. *J. Phys. Chem. B* **2009**, *113*, 11179−11185.
(21) Hong, S.; Leroueil, P. R.; Janus, E. K.; Peters, J. L.; Kober, M.-M.; Islam, M. T.; Orr, B. G.; Baker, J. R.; Holl, M. M. B. Interaction of polycationic polymers with supported lipid bilayers and cells: Nanoscale hole formation and enhanced membrane permeability. *Bioconjugate Chem.* **2006**, *17*, 728−734.
(22) Hong, S.; Hessler, J. A.; Banaszak Holl, M. M.; Leroueil, P.; Mecke, A.; Orr, B. G. Physical interactions of nanoparticles with biological membranes: The observation of nanoscale hole formation. *Chem. Health Saf.* **2006**, *13*, 16−20.
(23) Zuhorn, I. S.; Kalicharan, D.; Robillard, G. T.; Hoekstra, D. Adhesion receptors mediate efficient non-viral gene delivery. *Mol. Ther.* **2007**, *15*, 946−953.
(24) DiGioia, S.; Conese, M. Polyethylenimine-mediated gene delivery to the lung and therapeutic applications. *Drug Des., Dev. Ther.* **2008**, *2*, 163−188.
(25) Meng, Q.-H.; Robinson, D.; Jenkins, R. G.; McAnulty, R. J.; Hart, S. L. Efficient transfection of non-proliferating human airway epithelial cells with a synthetic vector system. *J. Gene Med.* **2004**, *6*, 210−221.
(26) Jett, M.; Jamieson, G. A. Comparison of binding sites for wheat germ agglutinin on Raji lymphoblastoid cells and their isolated nuclei and plasma membranes. *Biochemistry* **1981**, *20*, 5221−5226.
(27) Peters, B. P.; Ebisu, S.; Goldstein, I. J.; Flashner, M. Interaction of wheat germ agglutinin with sialic acid. *Biochemistry* **1979**, *18*, 5505−5511.
(28) Manders, E. M. M.; Stap, J.; Brakenhoff, G. J.; Driel, R. V.; Aten, J. A. Dynamics of three-dimensional replication patterns during the S-phase, analysed by double labelling of DNA and confocal microscopy. *J. Cell Sci.* **1992**, *103*, 857−862.
(29) Manders, E. M. M.; Verbeek, F. J.; Aten, J. A. Measurement of co-localizatin of objects in dual-colour confocal images. *J. Microsc.* **1993**, *169*, 375−382.
(30) Prevette, L. E.; Mullen, D. G.; Banaszak Holl, M. M. Polycation-induced cell membrane permeability does not enhance cellular uptake or expression efficiency of delivered DNA. *Mol. Pharmaceutics* **2010**, *7*, 870−883.
(31) DeWolf, H. K.; DeRaad, M.; Snel, C.; Steenbergen, M. J. v.; Fens, M. H. A. M.; Storm, G.; Hennink, W. E. Biodegradable poly(2-dimethylamino ethylamino)phosphazene for gene delivery to tumor cells. Effect of polymer molecular weight. *Pharm. Res.* **2007**, *24*, 1572−1580.
(32) Symonds, P.; Murray, J. C.; Hunter, A. C.; Debska, G.; Szewczyk, A.; Moghimi, S. M. Low and high molecular weight poly(L-lysine)s/poly(L-lysine)-DNA complexes initiate mitochondrial-mediated apoptosis differently. *FEBS Lett.* **2005**, *579*, 6191−6198.
(33) Shin, J.-Y.; Suh, D.; Kim, J. M.; Choi, H.-G.; Kim, J. A.; Ko, J. J.; Lee, Y. B.; Kim, J.-S.; Oh, Y.-K. Low molecular weight polyethylenimine for efficient transfection of human hematopoietic and umbilical cord blood-derived $CD34^+$ cells. *Biochim. Biophys. Acta* **2005**, *1725*, 377−384.
(34) Sundaram, S.; Lee, L. K.; Roth, C. M. Interplay of polyethyleneimine molecular weight and oligonucleotide backbone chemistry in the dynamics of antisense activity. *Nucleic Acids Res.* **2007**, *35*, 4396−4408.
(35) Brunner, S.; Sauer, T.; Carotta, S.; Cotten, M.; Saltik, M.; Wagner, E. Cell cycle dependence of gene transfer by lipoplex, polyplex and recombinant adenovirus. *Gene Ther.* **2000**, *7*, 401−407.
(36) Tait, A. S.; Brown, C. J.; Galbraith, D. J.; Hines, M. J.; Hoare, M.; Birch, J. R.; James, D. C. Transient production of recombinant proteins by chinese hamster ovary cells using polyethyleneimine/DNA complexes in combination with microtubule disrupting anti-mitotic agents. *Biotechnol. Bioeng.* **2004**, *88*, 707−721.
(37) Pack, D. W.; Hoffman, A. S.; Pun, S.; Stayton, P. S. Design and development of polymers for gene delivery. *Nat. Rev. Drug Discovery* **2005**, *4*, 581−593.
(38) Ogris, M.; Wagner, E. Targeting tumors with non-viral gene delivery systems. *Drug Discovery Today* **2002**, *7*, 479−485.
(39) Brunner, S.; Furtbauer, E.; Sauer, T.; Kursa, M.; Wagner, E. Overcoming the nuclear barrier: Cell cycle independent nonviral gene transfer with linear polyethylenimine or electroporation. *Mol. Ther.* **2002**, *5*, 80−86.
(40) Dean, D. A.; Strong, D. D.; Zimmer, W. E. Nuclear entry of nonviral vectors. *Gene Ther.* **2005**, *12*, 881−890.
(41) Lam, A. P.; Dean, D. A. Progress and prospects: nuclear import of nonviral vectors. *Gene Ther.* **2010**, *17*, 439−447.
(42) Thanaketpaisarn, O.; Nishikawa, M.; Okabe, T.; Yamashita, F.; Hashida, M. Insertion of nuclear factor-κB binding sequence into plasmid DNA for increased transgene expression in colon carcinoma cells. *J. Biotechnol.* **2008**, *133*, 36−41.
(43) Munkonge, F. M.; Amin, V.; Hyde, S. C.; Green, A.-M.; Pringle, I. A.; Gill, D. R.; Smith, J. W. S.; Hooley, R. P.; Xenariou, S.; Ward, M. A.; Leeds, N.; Leung, K.-Y.; Chan, M.; Hillery, E.; Geddes, D. M.; Griesenbach, U.; Postel, E. H.; Dean, D. A.; Dunn, M. J.; Alton, E. W. F. W. Identification and functional characterization of cytoplasmic determinants of plasmid DNA nuclear import. *J. Biol. Chem.* **2009**, *284*, 26978−26987.
(44) Breuzard, G.; Tertil, M.; Goncalves, C.; Cheradame, H.; Geguan, P.; Pichon, C.; Midoux, P. Nuclear delivery of NfκB-assisted DNA/polymer complexes: plasmid DNA quantification by confocal laser scanning microscopy and evidence of nuclear polyplexes by FRET imaging. *Nucleic Acids Res.* **2008**, *36*, e71.
(45) Dean, D. A. Import of plasmid DNA into the nucleus is sequence specific. *Exp. Cell Res.* **1997**, *230*, 293−302.

(46) Munkonge, F. M.; Dean, D. A.; Hillery, E.; Griesenbach, U. Emerging significance of plasmid DNA nuclear import in gene therapy. *Adv. Drug Delivery Rev.* **2003**, *55*, 749−760.
(47) Hebert, E. Improvement of exogenous DNA nuclear importation by nuclear localization signal-bearing vectors: a promising way for non-viral gene therapy? *Biol. Cell* **2003**, *95*, 59−68.
(48) Dean, D. A.; Dean, B. S.; Muller, S.; Smith, L. C. Sequence requirements for plasmid nuclear transport. *Exp. Cell Res.* **1999**, *253*, 713−722.
(49) Miller, A. M.; Dean, D. A. Tissue-specific and transcription factor-mediated nuclear entry of DNA. *Adv. Drug Delivery Rev.* **2009**, *61*, 603−613.
(50) Vacik, J.; Dean, B. S.; Zimmer, W. E.; Dean, D. A. Cell-specific nuclear import of plasmid DNA. *Gene Ther.* **1999**, *6*, 1006−1014.
(51) Prevette, L. E.; Lynch, M. L.; Reineke, T. M. Amide spacing influences pDNA binding of poly(amidoamine)s. *Biomacromolecules* **2010**, *11*, 326−332.
(52) Prevette, L. E.; Kodger, T. E.; Reineke, T. M.; Lynch, M. L. Deciphering the role of hydrogen bonding in enhancing pDNA-polycation interactions. *Langmuir* **2007**, *23*, 9773−9784.
(53) Orlov, S. N.; Aksentsev, S. L.; Kotelevtsev, S. V. Extracellular calcium is required for the maintenance of plasma membrane integrity in nucleated cells. *Cell Calcium* **2005**, *38*, 53−57.
(54) Zhou, Y.; Shi, J.; Cui, J.; Deng, C. X. Effects of extracellular calcium on cell membrane resealing in sonoporation. *J. Controlled Release* **2008**, *126*, 34−43.
(55) Reddy, A.; Caler, E. V.; Andrews, N. W. Plasma membrane repair is mediated by Ca+2-regulated exocytosis of lysosomes. *Cell* **2001**, *106*, 157−169.
(56) McNeil, P. L.; Kirchausen, T. An emergency response team for membrane repair. *Nat. Rev. Mol. Cell Biol.* **2005**, *6*, 499−505.
(57) Lam, A. M. I.; Cullis, P. R. Calcium enhances the transfection potency of plasmid DNA-cationic liposome complexes. *Biochim. Biophys. Acta* **2000**, *1463*, 279−290.
(58) Mozafari, M. R.; Omri, A. Importance of divalent cations in nanolipoplex gene delivery. *J. Pham. Sci.* **2007**, *96*, 1955−1966.
(59) Sun, Y.; Zeng, X.-R.; Wenger, L.; Cheung, H. S. Basic calcium phosphate cyrstals stimulate the endocytic activity of cells--inhibition by anti-calcification agents. *Biochem. Biophys. Res. Commun.* **2003**, *312*, 1053−1059.
(60) Kulkarni, V. I.; Shenoy, V. S.; Dodiya, S. S.; Rajyaguru, T. H.; Murthy, R. R. Role of calcium in gene delivery. *Expert Opin. Drug Delivery* **2006**, *3*, 235−245.
(61) Henle, K. J.; Moss, A. J.; Nagle, W. A. Mechanism of spermidine cytotoxicity at 37 degrees C and 43 degrees C in Chinese hamster ovary cells. *Cancer Res.* **1986**, *46*, 175−182.
(62) Wallace, H. M.; Fraser, A. V.; Hughes, A. A perspective of polyamine metabolism. *Biochem. J.* **2003**, *376*, 1−14.
(63) Seiler, N. Catabolism of polyamines. *Amino Acids* **2004**, *26*, 217−233.
(64) Seiler, N. Pharmacological aspects of cytotoxic polyamine analogues and derivatives for cancer therapy. *Pharmacol. Ther.* **2005**, *107*, 99−119.
(65) Regnestrom, K.; Ragnarsson, E. G. E.; Fryknas, M.; Koping-Hoggard, M.; Artursson, P. Gene expression profiles in mouse lung tissue after administration of two cationic polymers used for nonviral gene delivery. *Pharm. Res.* **2006**, *23*, 475−482.
(66) Beyerle, A.; Irmler, M.; Beckers, J.; Kissel, T.; Stoeger, T. Toxicity pathway focused gene expression profiling of PEI-based polymers for pulmonary applications. *Mol. Pharmaceutics* **2010**, *7*, 727−737.
(67) Nilsson, B. O. Biological effects of aminoguanidine: An update. *Inflamm. Res.* **1999**, *48*, 509−515.
(68) Takano, K.; Ogura, M.; Yoneda, Y.; Nakamura, Y. Oxidative metabolites are involved in polyamine-induced microglial cell death. *Neuroscience* **2005**, *134*, 1123−1131.